Path Construction and Visit Scheduling for Targets by Using Data Mules

Chih-Yung Chang, *Member, IEEE*, Gwo-Jong Yu, *Member, IEEE*, Tzu-Lin Wang, and Chih-Yu Lin

***Abstract*—In this paper, the target patrolling problem was considered, in which a set of mobile data collectors, known as data mules (DMs), must efficiently patrol a given set of targets. Because the time interval (or visiting interval) between consecutive visits to each target reflects the degree to which that target is monitored, the goal of this paper was to balance the visiting interval of each target. This paper first presents the basic target points patrolling algorithm, which enables an efficient patrolling route to be constructed for numerous DMs, such that the visiting intervals of all target points are stable. For scenarios containing weighted target points, a weighted target points patrolling (W-TPP) algorithm is presented, which ensures that targets with higher weights have higher data collection frequencies. The energy constraint of each DM was also considered, and this paper presents a W-TPP with recharge (RW-TPP) algorithm, which treats the energy recharge station as a weighted target and arranges for DMs to visit the recharge station before running out of energy. The performance results demonstrated that the proposed algorithms outperformed existing approaches in average visiting frequency, DM movement distance, average quality of monitoring satisfaction rate, and efficiency index.**

***Index Terms*—Disconnected targets, mobile data collectors, recharge station, weighted target, wireless sensor networks (WSNs).**

I. Introduction

WIRELESS sensor networks (WSNs) [1]–[10] have been used in many applications, including in environmental surveillance, scientific observation, and tracking. The coverage problem, which has been widely discussed in the literature, can be divided into three parts: the area, barrier, and target coverage problems. The area coverage problem is that any point in a given area must be covered by at least one sensor [11]–[13]. The barrier coverage problem is that the minimal number of sensors must be used to construct a barrier for detecting intruders crossing the given strip area [14]–[16]. In contrast to the area and barrier coverage problems, the target coverage problem refers to the fact that certain points in the monitoring area must be monitored by a set of active sensor nodes [17]–[23].

Reference [17] employed an integer linear programming solution to achieve the target coverage purpose. In [18], an algorithm was proposed that adopted disk and sector coverage models to determine the node density required for the monitoring region. Reference [19] investigated the placement of the minimal number of sensors required for each target to be covered by sensor nodes. In [17]–[19], algorithms have been proposed that required the deployment of a number of static sensors over the monitoring region to maintain network connectivity. However, in outdoor target points can be distributed over several disconnected areas. Deploying a large number of static sensors for the purpose of maintaining network connectivity can result in substantial hardware and maintenance costs. An alternative solution involves using mobile data collectors, which are also known as data mules (DMs). DMs visit all target points periodically to collect data, which are subsequently returned to the sink node.

References [20]–[23] have proposed heuristics for constructing patrolling routes enabling DMs to visit each target along a route. Reference [20] proposed centralized and distributed data collection mechanisms, called *CSweep* and *DSweep*. Since *CSweep* partitions the targets into several groups, a DM is assigned to each group that is responsible for executing the patrolling task for that group. *DSweep* enables each DM to locally determine its next visiting target based on information exchanged with other DMs. However, *DSweep* can be prone to constructing inefficient patrolling paths because no rule is proposed for cooperatively managing patrolling between various DMs. In addition, neither *CSweep* nor *DSweep* consider the recharging problem and the requirement that the monitoring quality of each target might be different. Furthermore, the visiting intervals (VIs) of each target might not be stable.

Similar to *CSweep*, CHB [21] is a centralized target patrolling mechanism. Each DM patrols constructed Hamilton circuits and periodically visits targets. However, the CHB mechanism does not consider the requirement of different monitoring quality and visiting frequency requirement. Furthermore, CHB also does not consider the recharging problem. In [22], sensors were divided into several groups, and a DM patrolled each group to perform data collection. The paper investigated the selection of appropriate locations, called polling points, for data collection. DMs were assigned to several polling points to maximize the sensing data that could be collected and balance the delay time between any two groups.

Manuscript received March 26, 2013; revised August 9, 2013; accepted December 13, 2013. Date of publication April 16, 2014; date of current version September 12, 2014. This work was supported by the National Science Council of the Republic of China under Contract NSC 100-2632-E-032-001-MY3 and Contract NSC 100-2221-E-007-054-MY3. This paper was recommended by Associate Editor N. Wu.

C.-Y. Chang and T.-L. Wang are with the Department of Computer Science and Information Engineering, Tamkang University, New Taipei City 25137, Taiwan (e-mail: cychang@mail.tku.edu.tw; tlwang@wireless.cs.tku.edu.tw).

G.-J. Yu is with the Department of Computer Science and Information Engineering, Aletheia University, New Taipei City 251, Taiwan (e-mail: yugj@mail.au.edu.tw).

C.-Y. Lin is with the Industrial Technology Research Institute, Hsinchu 31040, Taiwan (e-mail: rainlin@itri.org.tw).

Color versions of one or more of the figures in this paper are available online at http://ieeexplore.ieee.org.

Digital Object Identifier 10.1109/TSMC.2014.2314675

TABLE I
COMPARISON OF DATA COLLECTION MECHANISMS

Reference		Collection type	Path construction	Weighted targets	Recharge consideration	Stable visiting frequency
[17]		Sensor relay	N/A	×	N/A	N/A
[18]		Sensor relay	N/A	×	N/A	N/A
[19]		Sensor relay	N/A	×	N/A	N/A
[20]	*Dsweep*	Data Mule	×	×	×	×
	Csweep	Data Mule	×	×	×	×
CHB[21]		Data Mule	○	×	×	×
[22]		Data Mule	○	×	×	×
[23]		Data Mule	Predefined	×	×	×
The proposed *TCTP* mechanism		Data Mule	○	○	○	○

Each DM was assumed to be equipped with multiple antennas, and an SDMA coding mechanism was applied to the sensors' readings. However, the hardware support required by each DM in [22] is expensive.

Reference [23] assumed that the patrolling path (such as the bus trajectory) used by DM is predefined, and that DM periodically patrols path to conduct data collection. Sensors are partitioned into numerous clusters, and each cluster is assigned to a cluster header for executing data collection. To balance the energy consumption of each sensor, sensors closer to the bus trajectory must serve as relay nodes that forward sensing data to DM. In this approach, the relay nodes are treated as targets that must be visited by DM. However, Reference [23] does not consider the energy consumptions of cluster headers and relay nodes. In this system, cluster headers and relay nodes are likely to be exhausted earlier than other nodes, reducing the network lifetime.

In summary, above-mentioned researches did not consider the situation that the requirement of monitoring quality of each target might be different. In addition, most of them did not consider the requirement of stable VIs of each target. Furthermore, the recharge problem has been largely neglected. Table I compares the parameters of the data collection mechanisms presented in the literature; each column presents the considered parameters of the proposed TCTP compared with existing data collection mechanisms.

Similar to the network environments used in [20] and [21], a scenaio in which a set of target points (such as a fort, a powder room, and a marshal room) were distributed over a given region (such as a battlefield) was considered in this paper. This paper addressed the target patrolling problem, in which a set of DMs (such as robots or helicopters) must efficiently patrol a set of given targets. Based on [21], a basic target points patrolling (B-TPP) algorithm was proposed. The B-TPP algorithm considers the initial locations of all DMs, enabling an efficient patrolling route to be constructed such that the VIs of all target points can be minimized. For a scenario with various weighted targets (such as a powder room or a marshal room), a weighted target points patrolling (W-TPP) algorithm was proposed to enable targets with higher weight values to have higher data collection frequencies. By considering the energy constraint of each DM, a W-TPP with recharge (RW-TPP) algorithm was also proposed, which treated the recharge station as a weighted target and arranged for DMs to visit the recharge station before running out of energy. This paper complements existing references [20]–[23]. The contributions of this paper are listed as follows.

1) *Stable Visiting Frequency:* Most related studies have not considered that targets require stable visiting frequencies. Given targets with various weights, maintaining a stable visiting frequency for each target presents a considerable challenge. Each DM locally applies the proposed TCTP mechanism to globally maintain a stable visiting frequency for each target.
2) *Cooperative Target Visiting:* Each DM applying the proposed TCTP mechanism can cooperatively visit the targets to satisfy the monitoring quality of each target.
3) *Weighted Targets Have Higher Visiting Frequencies:* In the proposed TCTP mechanism, targets that have higher weights are visited more frequently to satisfy the monitoring requirements of those targets.
4) *Lower Moving Cost of Each DM Compared with Related Studies:* In the proposed TCTP mechanism, each DM systematically executes path construction by considering the weights of all targets so that it has the lowest moving cost as compared with the other target patrolling mechanisms.
5) *DM Recharging:* To support the perpetual operation of the network, the proposed TCTP mechanism considers the recharge problem. The recharge station is treated as a virtual target with a particular weight. The RW-TPP mechanism is proposed to manage the energy recharge problem.
6) *Extensive Simulations and Verification:* Extensive simulations in several scenarios were conducted to investigate the performance improvements gained using the proposed TCTP mechanism compared with existing state-of-the-art data collection mechanisms [20] and [21].

The remainder of this paper is organized as follows. Section II illustrates the network environment and presents the problem formulation. Sections III, IV, and V detail the B-TPP, W-TPP, and RW-TPP algorithms, respectively. Section VI compares the performance of the proposed algorithms with

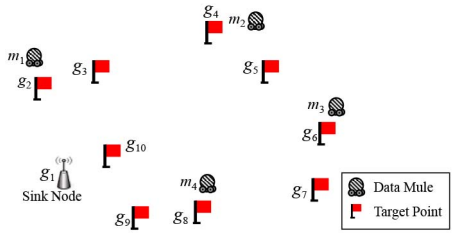

Fig. 1. Example of a number of targets and four DMs. The sink node is also treated as a target point, which should be visited by DMs.

that of existing algorithms. Finally, Section VII presents the conclusion.

II. Network Environment and Problem Formulation

This section introduces the network environment and the assumed characteristics of the given WSN. The problem formulation is subsequently presented.

A. Network Environment

This paper considered a scenario in which a set of target points was distributed over a given region. The target patrolling problem, in which a set of DMs (such as robots or helicopters) must efficiently patrol a set of given targets, was considered. The proposed network environment can be applied to a wide range of applications, for example, to battlefields, to direct robots or helicopters to periodically monitor a set of predefined targets, such as forts, powder rooms, or marshal rooms.

The terms $M = \{m_i \mid 1 \leq i \leq n\}$ and $G = \{g_i \mid 1 \leq i \leq h\}$ denote the DM set and target set, respectively. Fig. 1 presents an example of numerous targets and four DMs. As shown in this figure, DMs treated the sink node as a target point. Assume that each DM knows the numbers of DMs and targets and knows its own and all targets' location information. Furthermore, the moving speed and initial charge of all DMs were identical.

Since the importance of different targets might be different, a scenario was considered in which each target had a predefined weight value, which denoted the target's required visits within a certain time interval. In other words, a target with a higher weight value required more frequent visits by DMs. Let term w_i denote the weight value of target g_i. The weight value was assumed to be an integer. Furthermore, the number of important targets (such as powder rooms or marshal rooms) was assumed to be much lower than the number of general targets (such as general forts).

B. Problem Formulation

Given a set of DMs under energy constraints, this paper constructed efficient patrolling routes enabling DMs to visit all targets and collect information on those targets within a certain time period. Furthermore, the VIs of each target were required to be similar to ensure that the data update frequency for each target was stable. Let t_i^k denote the VI of target point g_i between the kth and $(k+1)$-th DM visit. Let $\overline{t_i}$ denote the average VI of target g_i and n represent the number of DMs. The value of $\overline{t_i}$ can be derived by applying (1)

$$\overline{t_i} = \frac{1}{n}\sum_{k=1}^{n} t_i^k. \tag{1}$$

Let h and V_i denote the number of target points and the standard deviation (SD) of the VIs of target g_i, respectively. Let V_s denote the SD of VIs of all targets, which can be calculated by applying (2), where $1 \leq i \leq h$

$$V_s = \frac{\sum_{i=1}^{h} V_i}{h}, \text{ where } V_i = \sqrt{\frac{1}{n}\sum_{k=1}^{n}\left(t_i^k - \overline{t_i}\right)^2}. \tag{2}$$

A low V_s value indicated that the VI for each target was more stable. To minimize the value of V_s, a patrolling route to satisfy (3) was investigated

$$\text{minimize}\,(V_s)\,. \tag{3}$$

Furthermore, a scenario in which targets had various weights was considered. Let T_{round} denote the time interval required for each DM to move along the constructed patrolling route once. Let N_i^{round} denote the number of DM visits received by target g_i during the time interval T_{round}. To ensure that targets with higher weight values had higher data collection frequencies, the proposed algorithm was expected to satisfy (4)

$$N_i^{\text{round}} = w_i, \text{ where } 1 \leq i \leq h. \tag{4}$$

Considering the energy constraint of each DM, this paper proposes a RW-TPP algorithm which, by treating the energy recharge station as a weighted target, ensures that DMs visit the recharge station before running out of energy. Let M^{Energy} denote the initial energy for each DM. Let l_i denote the path length patrolled by the DM m_i. Let c_m and c_s denote the energy consumption of each DM moving along a unit distance and collecting data from a single target, respectively. Let n_i denote the number of targets that have been visited by m_i. Let l_i^r denote the distance between m_i and the recharge station. This algorithm was proposed to ensure that DMs had sufficient remaining energies to reach the recharge station. Equation (5) expresses this constraint

$$M^{\text{Energy}} - [(l_i \times c_m) + (n_i \times c_s)] \geq l_i^r \times c_m. \tag{5}$$

Furthermore, because moving DMs to the recharge station involves additional energy consumption, another goal of the proposed algorithm was to ensure that DMs moved to the recharge station only when nearly depleted. In other words, as shown in (6), the remaining energy of a DM when it reaches the recharge station was minimized

$$\text{maximize}\left\{\left[(l_i + l_i^r) \times c_m\right] + (n_i \times c_s)\right\}. \tag{6}$$

III. Basic Target Points Patrolling Algorithm

This section presents the B-TPP algorithm, which was developed to balance the VIs for each target. The proposed B-TPP algorithm operates in two phases. In the first phase,

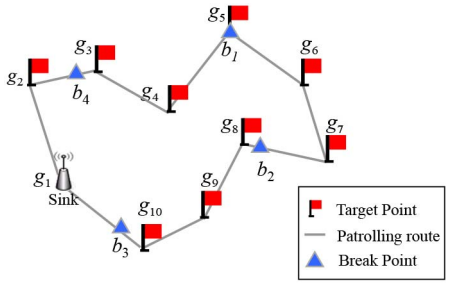

Fig. 2. Constructed patrolling path P starting from the sink node (also treated as a target) is $(g_i^P | 1 \leq i \leq 11)$ and the patrolling sequence is $g_1^P \rightarrow g_{10}^P \rightarrow g_9^P \rightarrow \ldots \rightarrow g_2^P \rightarrow g_1^P (= g_{11}^P)$.

all DMs individually construct the same patrolling path. Subsequently, in the second phase, each DM performs location initialization, and patrols the targets along the constructed patrolling path.

A. Path Construction

Determining the minimum distance required to pass each target is a *Euclidean traveling salesman problem*, which is an NP-hard problem [24]. To reduce the time required for constructing the path passing each target, the heuristic approach proposed in [21] was adopted to conduct DM path construction.

All DMs were aware of the locations of all targets. Therefore, based on the convex hull concept proposed in [21], all DMs were able to employ the same path construction rules and policies to individually construct the same patrolling path (a cycle passing each target exactly once and returning to the same start target). Let h denote the number of target points. Let $P = (g_i^P | 1 \leq i \leq h+1)$ denote the constructed patrolling path, where g_i^P denotes the ith visited target in path P in the counterclockwise direction. Notice that $g_1^P = g_{h+1}^P$ because P is a cycle. As shown in Fig. 2, the constructed patrolling path P starting from the sink node (also treated as a target) is $g_i^P | \ 1 \leq i \leq 11$ and the patrolling sequence is $g_1^P \rightarrow g_{10}^P \rightarrow g_9^P \rightarrow \ldots \rightarrow g_2^P \rightarrow g_1^P (= g_{11}^P)$.

B. Patrolling Strategy

As shown in (3), the value of V_s had to be minimized. To achieve this, this phase initiated the location of each DM by determining n breaking points and partitioning the constructed path into n segments with equal length. Each DM could move to one breaking point and start the patrolling task in conjunction with other DMs. Let g^{north} be the location of the northmost target. Let b_1 be the initial breaking point. The average distance d_{avg} of n segments is $|P|/n$, where $|P|$ denotes the length of path P. The n breaking points can be marked on path P every d_{avg} starting from the initial breaking point b_1. Let breaking points $b_1, b_2, b_3, \ldots, b_n$ be the labels of breaking points sequentially assigned from the initial breaking point in a clockwise direction. Each DM can construct n breaking points and then perform location initialization. In location initialization, each DM moves to the closest breaking point. If there is more than one DM at the same breaking point, the DM with a greater amount of remaining energy moves to the next breaking point along the constructed path P. These operations are repeatedly executed until each breaking point has only one DM.

As shown in Fig. 2, four DMs and a $|P|$ value of 58 m were assumed. Because the northmost target point g^{north} was g_5, it was treated as the initial breaking point b_1. All the other breaking points were labeled on path P every 58/4 m in a clockwise direction. Let m_{velocity} and T_{allocate} denote the moving velocity for each DM and the maximum time for allocating all DMs to the breaking points, respectively. Each DM measured the value of T_{allocate} by using

$$T_{\text{allocate}} = \frac{|P|}{M_{\text{velocity}}}. \tag{7}$$

After waiting the duration specified by T_{allocate}, each DM moved along path P to visit all targets. In addition, because the velocities of all DMs were identical, the VIs for each target were identical. Thus, the value of V_s was minimized.

IV. Weighted Target Points Patrolling Algorithm

This section further presents the distributed W-TPP algorithm, which enables targets with a higher weight value to have a higher data collection frequency. The proposed W-TPP algorithm operates in two phases. In the first phase, all DMs individually construct the same weighted patrolling path (WPP). Subsequently, each DM patrols the constructed WPP to visit all targets. The various types of target had different weight values, which were defined as follows.

Definition 1 (Normal Target Points and Very Important Points): If w_i equaled one, the target g_i was considered a normal target point (NTP)—an example of such a point is a general fort in a battlefield. Otherwise, the target was considered a very important point (VIP)—an example of such a point is a powder room or a marshal room in a battlefield.

The number of VIPs was far less than the number of NTPs. Furthermore, the difference between the weights of each VIP and NTP is not extremely large.

A. Path Construction

In this phase, a WPP was constructed. The path contained w_i distinct cycles intersecting at VIP g_i, such that VIP g_i was visited by a DM w_i times in each complete path traversal. The term C_i^f, the WPP, and the term f_i^k are defined as follows.

Definition 2 (Cycle C_i^f): Let $C_i^f = \left(g_k^f | 0 \leq k \leq q\right)$ denote the fth cycle passing the VIP g_i, where $1 \leq f \leq w_i$, and g_k^f represents the kth visited target starting from VIP g_i by a DM moving along C_i^f in a counterclockwise direction. Because C_i^f is a cycle, $g_0^f = g_q^f = g_i$.

As shown in Fig. 3, target g_4 is a VIP with weight value $w_4 = 2$. Two cycles

$$C_4^1 = \left(g_1^1, g_2^1, ..., g_7^1\right) = (g_4, g_3, g_2, g_1, g_{10}, g_9, g_4)$$
$$C_4^2 = \left(g_1^2, g_2^2, ..., g_6^2\right) = (g_4, g_8, g_7, g_6, g_5, g_4)$$

intersect at the VIP g_4. Because the patrolling path contains two cycles, the VIP g_4 is visited twice when a DM patrols the entire patrolling path.

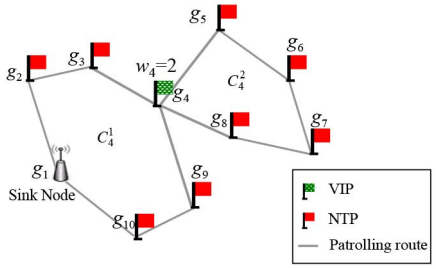

Fig. 3. Path $\overline{P} = (\overline{g}_k | 1 \le k \le 11)$ is a WPP because it satisfies Definition 3.

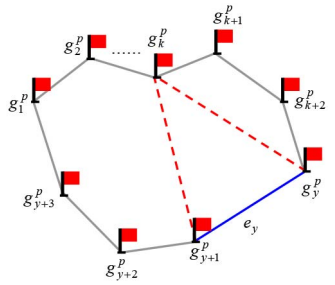

Fig. 4. Cycle construction process.

Definition 3 (Weighted Patrolling Path (WPP)): The path $\overline{P} = (\overline{g}_k | 1 \le k \le \sum_{i=1}^{h} w_i + 1)$ was considered to be a WPP if the following two criteria were satisfied.

1) For each $g_i \in \overline{P}$, exactly w_i cycles intersect at target g_i.
2) Path $\overline{P}$ is a cycle.

The term $\overline{g}_k$ denoted the kth target visited by a DM moving along path $\overline{P}$ in a counterclockwise direction.

As shown in Fig. 3, path $\overline{P}$ contains two cycles, C_4^1 and C_4^2, which intersect at the VIP g_4. Therefore, the VIP g_4 is visited twice when a DM completes a traversal of $\overline{P}$ once. Each NTP g_i is only intersected by a single cycle—either C_4^1 or C_4^2—where $i \in \{1, 2, 3, 5, 6, 7, 8, 9, 10\}$. Consequently, path $\overline{P} = (\overline{g}_k | 1 \le k \le 12) = (g_1, g_{10}, g_9, g_4, g_8, g_7, g_6, g_5, g_4, g_3, g_2, g_1)$ is a WPP.

As shown in (3), the VIs of all targets were required to be minimized and balanced. The VI f_i^k was defined as follows.

Definition 4: VI f_i^k

Let len_i^k denote the length of the kth cycle passing the VIP g_i. The kth VI for VIP g_i, f_i^k, can be measured using

$$f_i^k = \frac{len_i^k}{M_{\text{velocity}}}. \tag{8}$$

To minimize and balance the VIs for all targets, (9) must be satisfied

$$\min \left(\max_{1 \le i \le h, 1 \le k \le w_i} \left(f_i^k \right) \right). \tag{9}$$

The following describes how to construct the weighted patrolling path $\overline{P}$ by developing a distributed algorithm, which aims to satisfy Exp. (9). First of all, we consider the simple situation in which the number of VIPs is exactly one. After that, the situation of multiple VIPs will be discussed.

1) Single VIP Problem: The basic approach to constructing a WPP for the single VIP problem is described as follows. Initially, based on the convex hull concept proposed in [21], all DMs individually construct the same patrolling path $P = \left(g_i^P | 1 \le i \le h+1\right)$, which passes each target and then returns to the start target. Without loss of generality, let the kth target $g_k^P \in P$ in the patrolling path P be the VIP g_i. The cycle creation process is repeatedly executed by each DM until the number of created cycles, which intersect at the VIP g_i, is equal to the weight value w_i. The cycle creation process is introduced as follows.

The cycle creation process consists of two tasks: edge selection and cycle construction. First, as shown in Fig. 4, the break edge $e_y = \overline{g_y^P g_{y+1}^P}$, which connects the target points g_y^P and g_{y+1}^P in path P, is selected. Hereafter, the two targets g_y^P and g_{y+1}^P are referred to as break points. The cycle construction task subsequently removes edge e_y and connects the two break points g_y^P and g_{y+1}^P to VIP $g_k^P = g_i$ individually. Consequently, two cycles

$$C_i^1 = \left(g_k^P, g_y^P, ..., g_{k+2}^P, g_{k+1}^P, g_k^P\right)$$
$$C_i^2 = \left(g_k^P, ..., g_2^P, g_1^P, g_{y+3}^P, g_{y+2}^P, g_{y+1}^P, g_k^P\right)$$

intersect at VIP g_i. Cycle construction is repeatedly executed until w_i cycles intersect at the VIP g_i. Finally, the WPP $\overline{P}$ passes VIP g_i exactly w_i times, whereas the other NTP targets are visited exactly once.

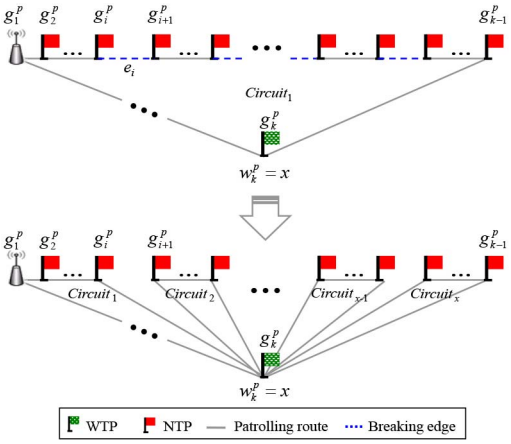

Fig. 5. Weighted-TPP patrolling route.

As shown in Fig. 5, cycle construction is repeatedly executed $x-1$ times. The newly constructed WPP $\overline{P}$ is composed of x cycles passing the VIP g_k^P. Whenever a DM moves along the WPP $\overline{P}$, the VIP g_k^P is visited x times. Thus, the data collection frequency of VIP g_k^P is x times that of NTPs.

The policy for selecting break edges determines the total length of the WPP $\overline{P}$ and the length of each newly formed cycle. Let target $g_k^P = g_k$ be a VIP in the constructed patrolling path P. Break edges are selected according to the balancing length policy, which balances the length of each cycle for VIP $g_k^P = g_i$ to ensure that the VIs for g_k^P are as similar as possible. Let $L^{\text{avg}} = |\overline{P}|/w_i$, where $|\overline{P}|$ denotes the length of path $\overline{P}$. The selected w_i cycles must satisfy (10), such that the maximal length of the created cycles approaches the value

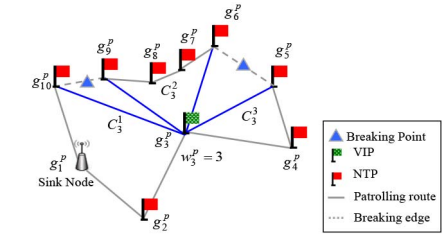

	$\lvert P\rvert$	$\lvert\overline{P}\rvert$	$\lvert C_3^1\rvert$	$\lvert C_3^2\rvert$	$\lvert C_3^3\rvert$
Path length	58	72	26	24	22

Fig. 6. Example of applying the balancing-length policy.

of L^{avg}. Consequently, the lengths of w_i cycles are similar

$$\min\left[\sum_{f=1}^{w_i}\left(\left|C_i^f\right| - L^{\text{avg}}\right)\right]. \tag{10}$$

Fig. 6 presents an example of the application of the balancing length policy. As shown in Fig. 6, the length of constructed patrolling path $|P|$ is 58 and the path length $|\overline{P}|$ yielded by applying the balancing length policy is 72. The increased path length is 14. The newly constructed cycles C_3^1, C_3^2, and C_3^3 intersect at the VIP g_3^P. The lengths of cycles C_3^1, C_3^2, and C_3^3 are 26, 24, and 22, respectively. Evidently, the lengths of the three cycles are similar and thus, the *VI*s are stable.

2) Multiple VIP Problem: The existence of multiple VIPs in the monitoring region is considered in this subsection. According to their weight values, each VIP g_i is assigned a priority value p_i. The cycle construction process is initiated by each DM for VIPs with higher priority before the other targets.

VIPs with higher weight values require the selection of more break edges to create more cycles and reflect their higher priority. Therefore, the priority p_i of VIP g_i is set by $p_i = w_i$. Fig. 7 depicts the procedure involved in constructing WPP $\overline{P}$. Let notation V denote the set of VIPs. As shown in Line 2 of Fig. 7, DMs construct the patrolling path P for each target point $g_i \in V$ until set V is empty. In Line 3, the same patrolling path P which passes all targets is initially constructed by all DMs individually. Subsequently, targets with higher weight values are prioritized in the cycle construction process. In Line 5, the DM identifies the target g_k with the highest weight value. Subsequently, in Lines 6–13, DMs construct several cycles intersecting the target g_k by applying the balancing length policy. Finally, the WPP is constructed by all DMs individually, as shown in Line 15.

B. Patrolling Strategy

Once the WPP $\overline{P}$ is constructed, each DM executes location initialization, as in the B-TPP algorithm. Each VIP g_i is intersected by w_i cycles, thus, all DMs follow the same patrolling rules in determining the traversal order for these cycles when they arrive at each VIP g_i. However, if two DMs have different traversal orders for the VIP g_i, the VIs of VIP g_i can be considerably uneven. Let S_i^w denote the set of targets that are connected to g_i in the WPP $\overline{P}$. The patrolling rule is proposed as follows.

Algorithm: Weighted Patrolling Path Construction
Input: A set of target points $G=\{g_1, g_2, \ldots g_h\}$, where h is the number of targets, and a set of *VIP*s V.
Output: *Weighted Patrolling Path* $\overline{P}$

1. **for** each *DM* **do**
2. **{while** $V \neq \phi$ **do**
3. {$P \leftarrow$**CyclicPath_Construct()**;
4. $\overline{P} \leftarrow P$;
5. $w_k \leftarrow \max(w_i)$;/* The target point g_k has the largest weights w_k. */
6. /* **BalancingLengthPolicy** */
7. **for** $x \leftarrow 1$ to $(w_k\text{-}1)$ **then**
8. Figure out the cycle C_k^f which satisfy Exp. (10), where $1 \le f \le w_k$.
9. $\overline{P} \leftarrow \overline{P} - \overline{g_y^P g_{y+1}^P}$;
10. $\overline{P} \leftarrow \overline{P} + \overline{g_y^P g_k^P}$;
11. $\overline{P} \leftarrow \overline{P} + \overline{g_{y+1}^P g_k^P}$;
12. **end for**
13. $V \leftarrow V - g_k$;
14. **end for**
15. **Return** $\overline{P}$ }}

Fig. 7. Procedure for constructing weighted patrolling path.

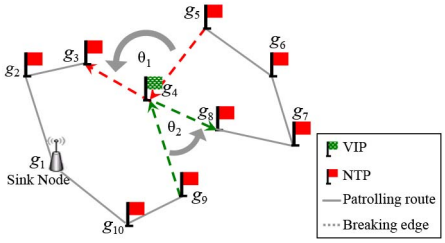

Fig. 8. Example of applying the proposed patrolling rule.

1) *Patrolling Rule:* When a DM arrives at a *VIP* g_i from a target g_j, it selects as its next target $g_k \in S_i^w$, which involves the smallest angle deviation from its former route g_j to g_i in the counterclockwise direction.

As shown in Fig. 8, when the DM moves from target g_5 to VIP g_4, it selects target g_3 as its next visiting target because $\overline{g_4 g_3}$ and $\overline{g_5 g_4}$ involve the smallest angle deviation θ_1 in the counterclockwise direction. Similarly, when the DM moves from target g_9 to VIP g_4, it selects g_8 as its next visiting target. Consequently, the constructed WPP $\overline{P}$ is (g_1, g_{10}, g_9, g_4, g_8, g_7, g_6, g_5, g_4, g_3, g_2, g_1).

V. Weighted Target Points Patrolling with Recharge Algorithm

DMs run on batteries that must be recharged at a recharge station. The RW-TPP algorithm, which considers energy recharge, was thus proposed. The basic concept in the RW-TPP is that the recharge station is treated as an NTP and all the targets are treated as VIPs. The RW-TPP operates in two phases: the *Path Construction Phase* and the *Patrolling Phase*. In the first phase, each DM individually constructs one path

for patrolling targets and another path for recharge. The second phase patrols the targets along one of the two constructed paths.

A. Path Construction

In this phase, each DM constructs two paths: the general patrolling path and the recharge patrolling path. The operations for constructing the WPP are similar to those defined in the W-TPP algorithm: the WPP $\overline{P}$ is constructed according to target weights. Furthermore, each DM constructs a weighted recharge path (WRP) which passes all targets plus the recharge station. When the remaining energy of a DM exceeds a certain threshold, the DM simply patrols the WPP $\overline{P}$ to visit all targets. Otherwise, the DM patrols along the WRP to achieve both the purposes of target patrolling and recharge.

Definition 5: WRP

The path $\overline{\overline{P}} = (\overline{\overline{g}}_k | 1 \le k \le \sum_{i=1}^{h} w_i + 2)$ is a WRP if it satisfies the following three criteria.

1) For each $g_i \in \overline{\overline{P}}$, exactly w_i cycles intersect at target g_i.
2) Path $\overline{\overline{P}}$ is a cycle.
3) The recharge station $R \in \overline{\overline{P}}$.

The term $\overline{\overline{g}}_i$ denotes the i-th visited target in path $\overline{\overline{P}}$in the counterclockwise direction.

Constructing a WRP is detailed as follows. Each DM first selects a break edge $e_y = \overline{\overline{g}_y \overline{g}_{y+1}}$ that satisfies (11), minimizing the length of the WRP. The two end points $\overline{g}_y$ and $\overline{g}_{y+1}$ are then individually connected to the recharge station R to form the new edges $\overline{\overline{g}_y R}$ and $\overline{\overline{g}_{y+1} R}$. Thus, the WRP $\overline{\overline{P}}$ passes all target points and the recharge station

$$\min_{1 \le i \le h} \left[\left(\left| \overline{\overline{g}_y R} \right| + \left| \overline{\overline{g}_{y+1} R} \right| \right) - \left| \overline{\overline{g}_y \overline{g}_{y+1}} \right| \right]. \tag{11}$$

B. Patrolling Strategy

In this phase, each DM determines its traversal path based on one of the constructed paths: $\overline{P}$ or $\overline{\overline{P}}$. Let M^{Energy} denote the initial energy of each DM. Each DM initially evaluates the patrolling round r by applying (12). The patrolling round r means that the DM is able to patrol all target r times along the $\overline{P}$ before energy depletion

$$r = \left\lfloor \frac{M^{\text{Energy}}}{\left(\left| \overline{P} \right| \times c_m \right) + (h \times c_s)} \right\rfloor. \tag{12}$$

This also means that each DM patrols along WRP $\overline{\overline{P}}$ every r rounds. If a DM has patrolled along the WPP $\overline{P}$ $r-1$ times, it patrols along the *WRP* $\overline{\overline{P}}$ in the next round to recharge.

The DM can recharge at any time if the moving cost of DM is not increased. In other words, if the recharge station is located on (or close to) the constructed path, the DM can recharge regardless of its remaining energy. However, when the recharge station is not located on the constructed path, the DM establishes an additional path for reaching the recharge station; hence, the recharging operation consumes greater energy and time.

Fig. 9 depicts the procedure for constructing the WRP $\overline{\overline{P}}$. As shown in Lines 2–3, each DM constructs the WRP $\overline{\overline{P}}$ based on the constructed WPP $\overline{P}$. To minimize the length of the WRP, as shown in Lines 4–7, the DM selects an appreciation break edge according to (11). Finally, the WRP $\overline{\overline{P}}$ is constructed by connecting the break points to the recharge station R, as shown in Line 9.

Algorithm: WRP Construction
Input: A set of target point $G=\{g_1, g_2, \ldots, g_h\}$, where h is the number of targets.
Output: *WRP* $\overline{\overline{P}}$

1. **for** each *DM* **do**
2. $\overline{P} \leftarrow$ ***W-TPP*_RouteConstruct();**
3. $\overline{\overline{P}} \leftarrow \overline{P}$
4. Figure out the edges $\overline{\overline{g}_y R}$ and $\overline{\overline{g}_{y+1} R}$ which satisfy Exp. (11), where $1 \le y \le h$.
5. $\overline{\overline{P}} \leftarrow \overline{\overline{P}} - \overline{\overline{g}_y \overline{g}_{y+1}}$;
6. $\overline{\overline{P}} \leftarrow \overline{\overline{P}} + \overline{\overline{g}_y R}$;
7. $\overline{\overline{P}} \leftarrow \overline{\overline{P}} + \overline{\overline{g}_{y+1} R}$;
8. **end for**
9. **Return** $\overline{\overline{P}}$

Fig. 9. Procedure of constructing WRP $\overline{\overline{P}}$.

VI. Performance Evaluation

The proposed TCTP algorithm was compared with a *Random* approach and with existing approaches [20], [21] in VI, the SD of the visiting interval, movement distance of each DM, and the DM energy efficiency. In the Random approach, unvisited targets were randomly selected as the next destination to construct a patrolling edge until all targets were visited.

Because none of the mechanisms to which the proposed mechanism was compared considered the weight of each target or the recharge problem, these mechanisms were modified to address these two concerns. The *CSweep* and CHB mechanisms were applied round-by-round. In each round, the *CSweep* and CHB mechanisms were used to construct a path passing each target. Subsequently, the weight of each target is reduced by one since the DM will visit each target once along the constructed patrolling path. At the end of the round, the target was removed if its weight was zero. Afterwards, *CSweep* and CHB were repeatedly applied in the next round to construct more paths and change the weight of each remaining target, until all targets were removed. In the *DSweep* mechanism, based on the exchanged information, the DM locally determined which target points to visit until the weights of all target points were satisfied. To compare the performance of the proposed W-TPP mechanism with the other mechanisms, the quality of monitoring (QoM) was defined. The weight w_i represents the QoM of target point g_i. That is, a g_i with weight w_i indicates that the target point g_i should have w_i visits within a given period of time.

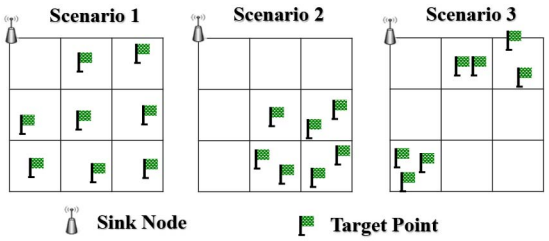

Fig. 10. Three scenarios are considered in the experiments.

A. Simulation Model

The following illustrates the parameters considered in the simulation environment. The velocity of eachDM was set at 2 m/s and the sensing range of each DM was set at 10 m. Receiving data from a target and moving a unit distance consumed energy at rates of 0.075 J/s and 8.267 J/m [25], respectively. The network size was 800 × 800 m, and the locations of the targets were randomly distributed throughout the monitoring region. The distance between every two targets was longer than the communication range (20 m) of a DM. Thus, the targets were disconnected in the experimental environment. In addition, the number of targets was dynamically adjusted, and the sink was treated as a target. Each simulation result was the average of 100 simulations. The 95% confidence interval was consistently lower than 5% of the reported values. To further investigate the performance of the three proposed mechanisms, three scenarios with three distinct target point arrangements were simulated. As shown in Fig. 10, the target points in Scenario 1 were distributed throughout the monitoring region. The target points in Scenario 2 were arranged close to each other but far from the sink node. In Scenario 3, the target points were divided into two groups, and the targets in each group were closed to each other.

B. Performance Study

The VI index denoted the average visiting intervals of all targets and was expressed as

$$VI = \frac{1}{h}\sum_{i=1}^{h}\overline{t_i}.$$

Fig. 11 compares VI indices of the proposed B-TPP algorithm with the *Random*, *DSweep*, *CSweep*, and *CHB* approaches in various scenarios. The simulation environment featured 25 targets with identical weights. VIs are reduced when greater numbers of DMs execute the target patrolling task along a given constructed path. Therefore, the value of the VI index generally decreases with an increasing number of DMs. This tendency is exhibited in Fig. 11(a)–(c). A high VI index value indicates that the constructed path is not efficient because the average distance between two consecutive DMs is long, increasing the average VI. The *Random* approach exhibited the highest VI index valueof all the cases, because it determining the next destination by randomly selecting unvisited targets. The *DSweep* approach exhibited the second highest VI index value of all the cases; in this approach, DMs locally determined the next visiting target point. The *CSweep* approach initially divided the DMs into several groups; subsequently, each DM individually patrols the targets of one group. Let sink edge denote the edge connecting the last visited target to the sink. Each DM applies *CSweep*, and must deliver the collected data to the sink node along the sink edge. Certain DMs must construct long paths if all targets in a group are far from the sink node. This lengthens the average length of sink edges constructed by all DMs. Thus, the *CSweep* approach also exhibited a higher VI index value than the CHB and B-TPP approaches in all cases. The CHB and the proposed B-TPP approaches yielded similar VI index values. Targets far from the sink node connected to targets that were closer to the sink node. Therefore, unlike the *CSweep* approach, the CHB and B-TPP approaches avoided the construction of long sink edges. Therefore, the lengths of the sink edges constructed using the CHB and B-TPP approaches were shorter than those constructed using the *CSweep* approach, and these approaches yielded lower VI index values. The proposed B-TPP approach yielded smaller value of VI index than CHB, because the B-TPP approach required each DM to execute location initialization to maintain the stable VIs between each target point. In general, the B-TPP outperformed the VI index values of the other four approaches in all cases.

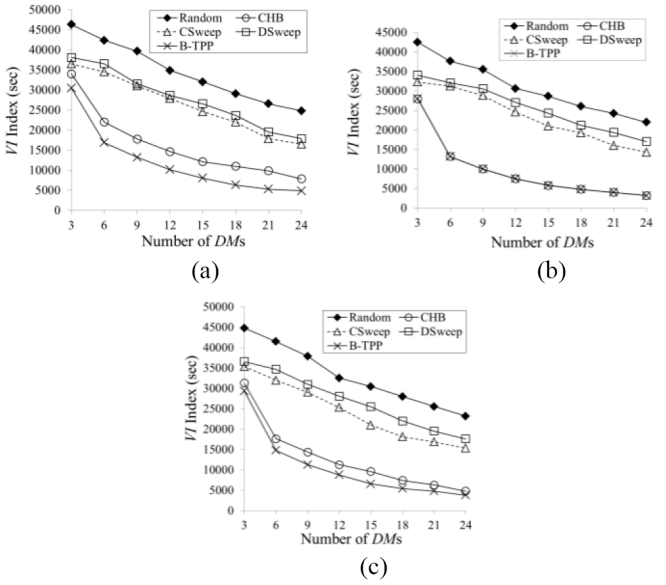

Fig. 11. Comparison of the *Random*, *CHB*, *DSweep*, *CSweep*, and *B-TPP* approaches in terms of VI index in three scenarios. The weights of all targets are identical. (a) Scenario 1. (b) Scenario 2. (c) Scenario 3.

Figs. 12 and 13 compare the performance of the proposed W-TPP algorithm and the other four approaches regarding the VI index and SD, respectively. There are five VIPs out of 25 targets in the networks and the weights of VIPs are set to 3.

As shown in Fig. 12, a target was randomly selected to observe its VI value. The Random approach, which randomly selected the next target to be visited, exhibited VI index values that changed considerably between scenarios. In *DSweep*, each DM locally determined the next visited target point until the QoMs of all target points were satisfied, resulting in lengthy patrolling paths. Consequently, the *DSweep* yielded a higher VI index value than did the *CSweep*, *CHB*, and *W-TPP*

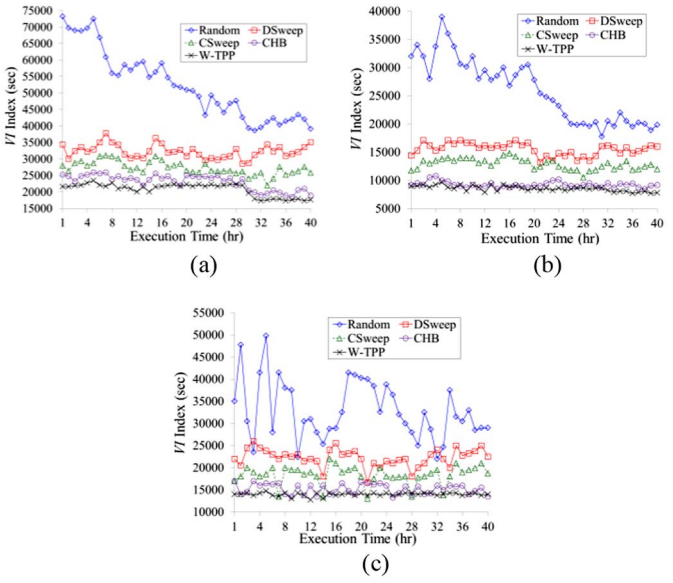

Fig. 12. Comparison of the *Random*, *CHB*, *DSweep*, *CSweep*, and the proposed *W-TPP* approaches in terms of *VI* index. (a) Scenario 1. (b) Scenario 2. (c) Scenario 3.

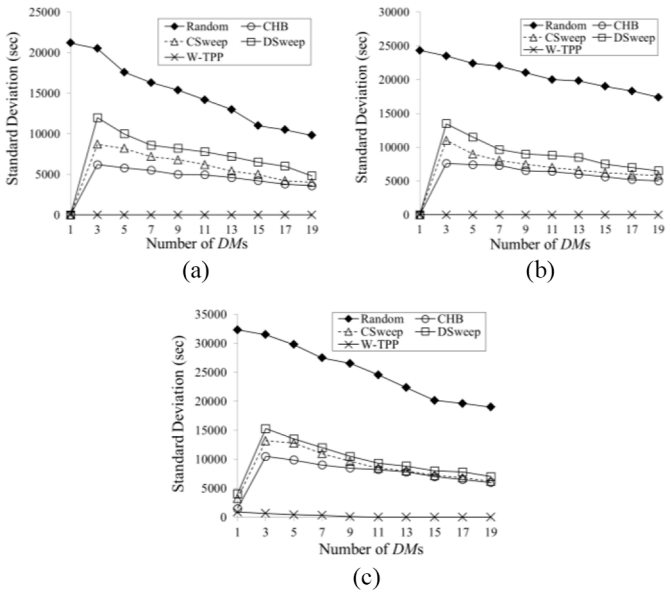

Fig. 13. Comparison of the *Random*, *CHB*, *DSweep*, *CSweep*, and the proposed *W-TPP* approaches in terms of *SD*. (a) Scenario 1. (b) Scenario 2. (c) Scenario 3.

approaches in all cases. In the *CSweep* and *CHB* approaches, each path constructed in a round contained a distinct number of targets. Hence, the lengths of the constructed patrolling paths differed, leading to unstable VI index values. Moreover, DMs applying the *CSweep* and *CHB* approaches constructed longer sink edges, resulting in higher VI values compared with the proposed W-TPP algorithm. This is because the proposed W-TPP mechanism applies the proposed balancing length policy. All DMs patrol targets along the same constructed patrolling path. Therefore, the curve of the proposed W-TPP algorithm was much more stable than those of the other four approaches in all cases. Overall, the proposed W-TPP algorithm outperformed the *Random*, *DSweep*, *CSweep*, and *CHB* approaches regarding VI index values.

To further investigate the impact of locations of target points on VIs of target points, the following defines the standard deviation, called SD_i, for a single target g_i. The SD_i is formulated as

$$SD_i = \sqrt{\frac{1}{n}\sum_{k=1}^{n}(t_i^k - \overline{t_i})^2}.$$

A low SD_i value indicated that the VIs of target point g_i were similar, and thus, the data collection frequency was stable.

As shown in Fig. 13, a target was randomly selected to observe its SD value. In general, the curves of all five compared mechanisms decreased with an increasing number of DMs. The primary reason for this is that a large number of DMs can share the interval lengths, leading to lower SD values. As indicated by Fig. 12, the Random approach yielded the highest SD value of all scenarios because DMs using the *Random* approach constructed the longest patrolling paths. In *DSweep*, each DM locally exchanged information with other DMs to determine the next target, leading to the construction of inefficient patrolling paths. Consequently, the *DSweep* approach yielded a higher SD value than the *CSweep*, *CHB*, and *W-TPP* approaches did. The *CSweep* and *CHB* approaches yielded longer sink edges, resulting in longer patrolling paths and higher SD values compared with the proposed W-TPP algorithm. By applying the balancing length policy, the SD value of the proposed W-TPP mechanism was maintained constant. In general, the proposed W-TPP algorithm exhibited more favorable network performance than the *Random*, *DSweep*, *CSweep*, and *CHB* approaches regarding the SD value.

Fig. 14 compares the DM movement distance of each of the five approaches. Scenario 2 had the shortest average distance between targets, thus, all the patrolling mechanisms had the shortest movement distances in Scenario 2, as shown in Fig. 14(b). In all cases, the DMs using the *Random* approach constructed the most inefficient path, leading to the longest movement distance. The movement distance of DMs using the CHB approach was longer than those of DMs using the *CSweep* and *DSweep* approaches. This is because the average sink edge of paths constructed using the CHB approach might have been longer than the average sink edge constructed using the *CSweep* and *DSweep* approaches. DMs using the proposed W-TPP approach constructed the shortest patrolling path, with the shortest sink edge length, while satisfying the QoMs of all target points. Consequently, the proposed W-TPP mechanism outperformed the other four patrolling mechanisms regarding movement distance in all cases, as shown in Fig. 14.

Fig. 15 shows the average QoM satisfaction rates, denoted by ϑ, yielded by applying the five patrolling mechanisms under various time constraints and with various numbers of VIPs. The number of VIPs was set to 5, 10, and 15 out of 25 targets, and the results are shown in Fig. 15(a)–(c),

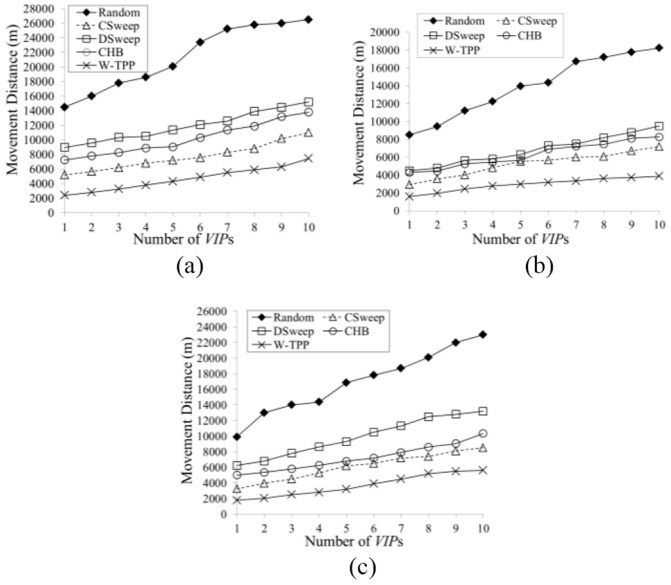

Fig. 14. Comparison of the *Random*, *CHB*, *DSweep*, *CSweep*, and *W-TPP* in terms of moving cost. (a) Scenario 1. (b) Scenario 2. (c) Scenario 3.

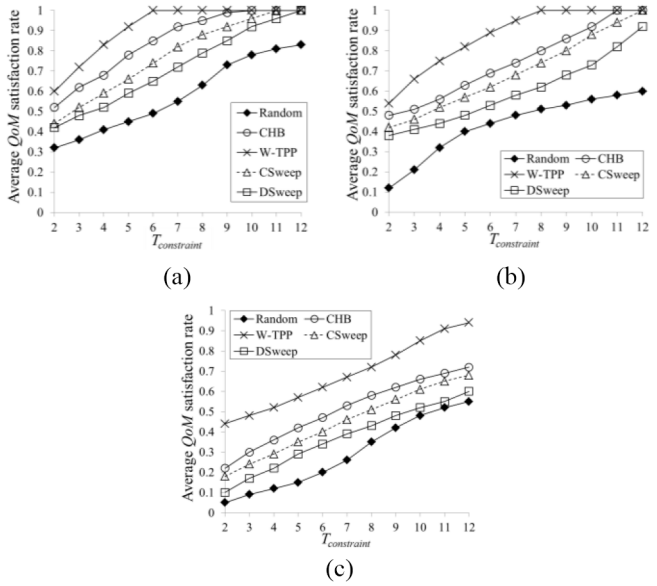

Fig. 15. Average QoM satisfaction rate by applying the five patrolling mechanisms with different time constraints and number of VIPs. (a) 5 VIPs. (b) 10 VIPs. (c) 15 VIPs.

respectively. The QoM of each target point was required to be satisfied within the given time constraint $T_{\text{constraint}}$. A high value of $T_{\text{constraint}}$ indicated that each DM had more time to execute the patrolling task, hence, the QoM of each target could be satisfied with a higher probability. Let f_i' denote the number of visits of target g_i in a given $T_{\text{constraint}}$. The average QoM satisfaction rate ϑ can be measured according to

$$\vartheta = \left(\sum_{i=1}^{h} f_i^{'}\right) \Big/ \left(\sum_{i=1}^{h} w_i\right). \tag{13}$$

A high value of ϑ indicated that the QoM of each target could be satisfied within a given $T_{\text{constraint}}$. In general, the curves of all five patrolling mechanisms are increased with increasing $T_{\text{constraint}}$ values. The *Random* mechanism yielded the lowest ϑ value in all cases. By contrast, the proposed W-TPP mechanism yielded the highest ϑ value because it enabled DMs to construct patrolling paths based on the weight of each target. As shown in Fig. 16, the proposed W-TPP mechanism outperformed the other four patrolling mechanisms regarding the average QoM satisfaction rate in all cases.

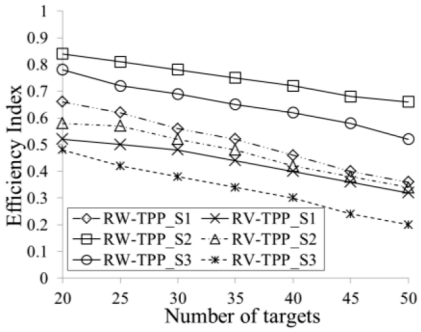

Fig. 16. Comparison of the proposed RW-TPP and RV-TPP mechanisms in terms of efficiency index by varying the number of targets. The recharge station is located at the opposite side of sink node in three scenarios.

To manage the recharge problem, the recharge station can be treated as a target which must be visited by the DMs running low on energy. Fig. 16 displays the efficiency of the proposed RW-TPP mechanism. As shown in Fig. 16, 10 of the 50 targets were VIPs, and the weight value of each VIP was set to 3. Three scenarios were considered in the simulation, and the recharge station was located at the opposite side of sink node. The RW-TPP_S1 approach denotes the results obtained by applying the RW-TPP in Scenario 1. Let ζ denote the total energy consumption of all DMs patrolling all paths in each round. The energy consumption efficiency of the DMs was measured according to the efficiency index

$$\text{Efficiency index} = \left(\sum_{i=1}^{h} w_i\right) \Big/ \zeta.$$

The proposed RW-TPP mechanism was compared with the RV-TPP approach, which was modified based on W-TPP. More specifically, in the RV-TPP approach, the recharge station was treated as a target with a weight of 1 and the W-TPP approach was applied to construct a patrolling path. In each round of the RV-TPP approach, the QoMs of all targets were satisfied by the constructed patrolling path, even though the DM continued to retain sufficient energy. Unnecessary visits to the recharging station resulted in additional energy consumption, reducing efficiency index values. Using the proposed RW-TPP algorithm, each DM initially calculated the maximal number of rounds, r, which its energy could support, as shown in (12). The weight w_i of all targets g_i should be changed by $r \times w_i$, and the weight of the recharge station was set to 1. Subsequently, the W-TPP approach was applied by each DM to construct a patrolling path. Consequently, the recharge station was visited by DMs only when their remaining energies were insufficient to finish traveling the entire patrolling path. Consequently, the proposed RW-TPP outperformed the RV-TPP approach in all cases regarding efficiency index values.

In summary, the number of DMs, the number of VIPs, and various scenarios were considered to evaluate the performance of the proposed approach. VI values decrease with an increasing number of DMs, because VI values are highly dependent on the length of the patrolling path of each DM. Reducing the number of DMs increases the average patrolling path of each DM, resulting in a high VI value. In addition, the number of VIPs affects the average QoM satisfaction rate. To reflect the unequal importance of VIPs and NTPs, VIPs require more edges that pass them, increasing the movement distance of each DM. Because increasing the movement distance of each DM results in a lower visiting frequency for each target, the average QoM satisfaction rate is reduced when the number of VIPs is increased. Finally, the locations of the sink and the targets also affect the performance of the proposed TCTP mechanism. Separating the sink and the targets lengthens the patrolling paths, resulting in higher VI index values, and longer DM movement distances.

VII. Conclusion

This paper proposes a B-TPP algorithm aiming at constructing an efficient patrolling path along which all DMs can patrol each target with stable VIs. A W-TPP algorithm was proposed to enable VIP targets, which have higher weights than other targets, to be visited more frequently in each round. Considering the energy constraint of each DM, the RW-TPP algorithm was proposed; the RW-TPP algorithm treats the recharge station as a weighted target and arranges for all DMs to visit the recharge station before running out of energy. The performance of the proposed algorithms was evaluated, and the results demonstrated that the proposed TCTP mechanism outperformed existing approaches [20] and [21] regarding SD value, average visiting frequency, DM movement distance, average QoM satisfaction rate, and efficiency index.

Acknowledgment

The authors would like to thank C.-Y. Hsieh for his contribution.

References

[1] M. P. Kolba, W. R. Scott, Jr., and L. M. Collins, "A framework for information-based sensor management for the detection of static targets," *IEEE Trans. Syst., Man, Cybern. A, Syst. Humans,* vol. 41, no. 1, pp. 105–120, Jan. 2011.

[2] C. Giovannangeli and P. Gaussier, "Interactive teaching for vision-based mobile robots: A sensory-motor approach," *IEEE Trans. Syst., Man, Cybern. A, Syst. Humans,* vol. 40, no. 1, pp. 13–28, Jan. 2010.

[3] F. Alonso-Fernandez, J. Fierrez, D. Ramos, and J. Gonzalez-Rodriguez, "Quality-based conditional processing in multi-biometrics: Application to sensor interoperability," *IEEE Trans. Syst., Man, Cybern. A, Syst. Hum.*, vol. 40, no. 6, pp. 1168–1179, Nov. 2010.

[4] D. Gu, "A game theory approach to target tracking in sensor networks," *IEEE Trans. Syst., Man, Cybern. B, Cybern.*, vol. 41, no. 1, pp. 2–13, Feb. 2011.

[5] S. Ferrari, G. Zhang, and T. A. Wettergren, "Probabilistic track coverage in cooperative sensor networks," *IEEE Trans. Syst., Man, Cybern. B, Cybern.*, vol. 40, no. 6, pp. 1492–1504, Dec. 2010.

[6] C. Y. Chang, J. P. Sheu, and Y. C. Chen, "An obstacle-free and power efficient deployment algorithm for wireless sensor networks," *IEEE Trans. Syst., Man, Cybern. A, Syst. Humans,* vol. 39, no. 4, pp. 795–806, Jul. 2009.

[7] W. Zhang, Q. Yin, H. Chen, F. Gao, and N. Ansari, "Distributed angle estimation for localization in wireless sensor networks," *IEEE Trans. Wireless Commun.*, vol. 12, no. 2, pp. 527–537, Feb. 2013.

[8] D. Akselrod, A. Sinha, and T. Kirubarajan, "Information flow control for collaborative distributed data fusion and multisensor multitarget tracking," *IEEE Trans. Syst., Man, Cybern. C, Appl. Rev.*, vol. 42, no. 4, pp. 501–517, Jul. 2012.

[9] Y. Lin *et al.*, "An ant colony optimization approach for maximizing the lifetime of heterogeneous wireless sensor networks," *IEEE Trans. Syst., Man, Cybern. C, Appl. Rev.*, vol. 42, no. 3, pp. 408–420, May 2012.

[10] C. Y. T. Ma, D. K. Y. Yau, N. K. Yip, N. S. V. Rao, and J. Chen, "Stochastic steepest descent optimization of multiple-objective mobile sensor coverage," *IEEE Trans. Veh. Technol.*, vol. 61, no. 4, pp. 1810–1822, May 2012.

[11] A. Ababnah and B. Natarajan, "Optimal control-based strategy for sensor deployment," *IEEE Trans. Syst., Man, Cybern. A, Syst. Humans,* vol. 41, no. 1, pp. 97–104, Jan. 2011.

[12] C. Liu, K. Wu, Y. Xiao, and B. Sun, "Random coverage with guaranteed connectivity: Joint scheduling for wireless sensor networks," *IEEE Trans. Parallel Distrib. Syst.*, vol. 17, no. 6, pp. 562–575, Jun. 2006.

[13] Z. Yun, X. Bai, D. Xuan, T. H. Lai, and W. Jia, "Optimal deployment patterns for full coverage and k-connectivity ($k \leq 6$) wireless sensor networks," *IEEE/ACM Trans. Netw.*, vol. 18, no. 3, pp. 934–947, Jun. 2010.

[14] A. Chen, S. Kumor, and T. H. Lai, "Designing localized algorithms for barrier coverage," in *Proc. ACM MobiCom*, Montreal, QC, Canada, Sep. 2007.

[15] A. Chen, T. H. Lai, and D. Xuan, "Measuring and guaranteeing quality of barrier-coverage in wireless sensor networks," in *Proc. ACM MobiHoc*, Hong Kong, May 2008.

[16] D. Dash, A. Bishnu, A. Gupta, and S. C. Nandy, "Approximation algorithms for deployment of sensors for line segment coverage in wireless sensor networks," *Wireless Netw.* vol. 19, no. 5, pp. 857–870. Sep. 2012.

[17] K. Chakrabarty, S. Iyengar, H. Qi, and E. Cho, "Grid coverage for surveillance and target location in distributed sensor networks," *IEEE Trans. Comput.*, vol. 51, no. 12, pp. 1448–1453, Dec. 2002.

[18] W. Wang, V. Srinivasan, B. Wang, and K. C. Chua, "Coverage for target localization in wireless sensor networks," *IEEE Trans. Wireless Commun.*, vol. 7, no. 2, pp. 667–676, Feb. 2008.

[19] G. J. Fan, F. Liang, and S. Y. Jin, "An efficient approach for point coverage problem of sensor network," in *Proc. IEEE ISECS*, Guangzhou, China, 2008.

[20] M. Li *et al.*, "Sweep coverage with mobile sensors," *IEEE Trans. Mobile Comput.*, vol. 10, no. 11, pp. 1534–1545, Nov. 2011.

[21] F. J. Wu and Y. C. Tseng, "Energy-conserving data gathering by mobile mules in a spatially separated wireless sensor network," *Wireless Commun. Mobile Comput.* vol. 13, no. 15, pp. 1369–1385, Oct. 2011.

[22] M. Zhao, M. Ma, and Y. Yang, "Efficient data gathering with mobile collectors and space-division multiple access technique in wireless sensor networks," *IEEE Trans. Comput.*, vol. 60, no. 3, pp. 400–417, Mar. 2011.

[23] C. Konstantopoulos, G. Pantziou, D. Gavalas, A. Mpitziopoulos, and B. Mamalis, "A rendezvous-based approach enabling energy-efficient sensory data collection with mobile sinks," *IEEE Trans. Parallel Distrib. Syst.*, vol. 23, no. 5, pp. 809–817, May 2012.

[24] M. Al-Mulhem and T. Al-Maghrabi, "Efficient convex-elastic net algorithm to solve the Euclidean traveling salesman problem," *IEEE Trans. Syst., Man, Cybern. B, Cybern.*, vol. 28, no. 4, pp. 618–620, Aug. 1998.

[25] S. Ganeriwal, A. Kansal, and M. B. Srivastava, "Self-aware actuation for fault repair in sensor networks," in *Proc. IEEE ICRA*, New Orleans, LA, USA, Apr. 2004.

Chih-Yung Chang (M'05) received the Ph.D. degree in computer science and information engineering from National Central University, Zhongli, Taiwan, in 1995.

He is currently a Full Professor with the Department of Computer Science and Information Engineering at Tamkang University, New Taipei, Taiwan. His current research interests include Internet of things, wireless sensor networks, ad hoc wireless networks, and LTE broadband technologies.

Dr. Chang has served as an Associate Guest Editor for many SCI-indexed journals, including the *International Journal of Ad Hoc and Ubiquitous Computing* (IJAHUC) in 2011–2014, *International Journal of Distributed Sensor Networks* (IJDSN) in 2012–2014, *IET Communications* in 2011, *Telecommunication Systems* (TS) in 2010, *Journal of Information Science and Engineering* (JISE) in 2008, and *Journal of Internet Technology* (JIT) during 2004 and 2008. He was an Area Chair of IEEE AINA'2005, TANET'2000, TANET'2010, IEEE WisCom'2005, EUC'2005 IEEE ITRE'2005, and IEEE AINA 2008, Program Co-Chair of IEEE MNSA'2005, UbiLearn'2006, WASN'2007, ACM SAMnet'2008, IEEE AHUC'2008, iCube'2010, iCube'2011, Workshop Co-Chair of MSEAT'2003, MSEAT'2004, IEEE INA'2005, ICS'2008, NCS'2009, IEEE VCNA'2009, and Publication Chair of MSEAT'2005 and SCORM'2006.

Gwo-Jong Yu (M'03) received the B.S. degree in computer science from Christian University, Zhongli, Taiwan, in 1989, and the Ph.D. degree in computer science from the National Central University, Zhongli, Taiwan, in 2001.

Since August 2001, he was with the Faculty of Department of Computer Science and Information Engineering (CSIE), Aletheia University, New Taipei, Taiwan. He became a Professor at the Department of CSIE, Aletheia University, in 2011. His current research interests include wireless sensor networks, ad hoc networks, WiMAX, and LTE.

Tzu-Lin Wang received the B.S. and M.S. degrees in computer science and information engineering from Aletheia University, New Taipei, Taiwan, in 2007 and 2009, respectively. She is currently pursuing the Ph.D. degree with the Department of Computer Science and Information Engineering at Tamkang University, New Taipei, Taiwan.

Her current research interests include wireless sensor networks, ad hoc wireless networks, mobile/wireless computing, and WiMAX.

Ms. Wang has won numerous scholarships in Taiwan and has participated in many wireless sensor networking projects.

Chih-Yu Lin received the B.S. degree in computer science and information engineering from Aletheia University, New Taipei, Taiwan, in 2007, and the M.S. and Ph.D. degrees in computer science and information engineering from Tamkang University, New Taipei, Taiwan, in 2009 and 2012, respectively.

He is currently with the Industrial Technology Research Institute, Taiwan.

Dr. Lin has received several scholarship grants in Taiwan and has participated in many wireless sensor network projects.